Heavy metals retention (Pb(II), Cd(II), Ni(II)) from single and multimetal solutions by natural biosorbents from the olive oil milling operations

Heavy metals retention (Pb(II), Cd(II), Ni(II)) from single and multimetal solutions by natural biosorbents from the olive oil milling operations

Andrea Petrella[a], Danilo Spasiano[a], Pasquale Acquafredda[c], Nicoletta De Vietro[b], Ezio Ranieri[a], Pinalysa Cosma[b], Vito Rizzi[b], Valentina Petruzzelli[a], Domenico Petruzzelli[a]

[a]Dipartimento di Ingegneria Civile, Ambientale, Edile, del Territorio e di Chimica, Politecnico di Bari, Via E. Orabona, 4, 70125, Bari, Italy

[b]Dipartimento di Chimica, Università degli Studi di Bari "Aldo Moro", Via E. Orabona, 4, 70125, Bari, Italy

[c]Dipartimento di Scienze della Terra e Geoambientali, Università degli Studi di Bari "Aldo Moro", Via E. Orabona, 4, 70125, Bari, Italy

* Corresponding author: Tel.+39(0)805963275, Fax +39(0)805963635,
e-mail: andrea.petrella@poliba.it

Abstract. In the present paper, the lignocellulosic residues from the olive oil industry in South-East Italy, namely BOP (Biosorbent from Oil Production), were used as sorbents for heavy metals retention (Pb^{+2}, Cd^{+2}, Ni^{+2}) in water and wastewater treatments.

To the purpose, thermodynamic and kinetic investigations for single and multispecies systems were carried-out through batch equilibrium isotherms and column dynamic experiments.

In the case of batch tests, maximum metals retentions (q_{max}) in single ion solutions were 22.4 mg/g_{BOP}, 10.5 mg/g_{BOP}, 5.04 mg/g_{BOP} respectively for Pb^{+2}, Cd^{+2} and Ni^{+2}, lower figures were detected in the case of ternary systems with values exceeding 10.51 mg/g_{BOP}, 5.11 mg/g_{BOP}, 3.81

mg/g_{BOP} respectively. Further drastic reductions were detected in tap water. Langmuir and Freundlich isotherms led to good correlations of the data in single-ion and ternary solutions in demineralized water. Freundlich isotherms gave better correlation in tap water.

In the case of column tests, operating capacities resulted in the same order with Pb^{+2}> Cd^{+2} > Ni^{+2}. After retention, the exhausted metal converted materials were included into cement conglomerates for a possible employment in the building industry applications, thus minimizing their potential environmental impact.

Keywords: Olive waste; Sorption; Porous media; Batch reactor; Column dynamic experiment; Wastewater treatment

1.Introduction

Biosorption relies on the use of natural residues from the agro-food industry to remove organic and inorganic pollutants present in wastewater of different nature and origin (Abdolali et al., 2014; Ahmad et al., 2017; Ashraf et al., 2017; Çifçi, and Meriç, 2016; Fomina and Gadd, 2014; Ismail et al., 2017; Jafar Ahamed et al., 2017; Kahn et al., 2017; Michalak et al., 2013). Among vegetal waste materials, husks from: a) the olive oil milling operations (Doyurum and Çelik; 2006; El-Kady et al.; 2016; Ronda et al., 2016); b) wheat and maize crops (Mosa et al., 2016; Qi et al., 2016); c) plant root tissues (Chiarantini et al., 2016; Rezania et al., 2016); d) fruit residues (Ahmad et al., 2016; do Nascimento et al., 2016) are widespread in all the Mediterranean areas. Above wastes result to be particularly versatile toward removal of biopersistent pollutants from wastewater due to their low cost (if any), ready availability and eco-compatibility at large, thus representing a valuable alternative to conventional sorption technologies from both technical and economic points of view (do Nascimento et al., 2016; Qi et al., 2016; Rezania et al., 2016). Other advantages are associated with their high efficiency, already at very low concentrations (µg/L), no production of toxic sludge

after conventional precipitation and, above all, the possibility of recovery energy and valuable materials after burning down of the exhausted sorbents (Chouchene et al., 2014; Fernández-Pereira et al., 2011).

In the present paper, the retention (sorption) of biopersistent pollutants from industrial wastewater was obtained by the use of biosorbents from the olive oil milling operations (pressing and chemical extraction), namely BOP (Biosorbent from Oil Production), deriving from the South-East Italy. Specifically, BOP residues include partially decomposed lignocellulosic materials from peel and olives kernel. The solid fraction is characterized by a carbohydrate (cellulosic) backbone including carboxylic and phenolic functional groups (Baccar et al., 2009; Chao and Chang, 2012; Konstantinou et al., 2007; Martín-Lara et al., 2009). Due to the substantially high transport and disposal costs of these wastes, the high water content which does not allow for their direct landfilling and the low revenues from the olive oil production, reuse of the reference materials is almost imperative for best economic management of the waste. Specifically, 75% of the annual worldwide production of olive oil comes from European Union countries around the Mediterranean Sea (average olive harvest of 10^7 tons per year). Considering that the demand of olive oil is rapidly increasing, environmental pollution due to olive mill liquid and solid wastes is a growing problem especially in the Mediterranean region. In fact, after the processing of 1 ton of olive, 200 kg of oil are produced with 600-1200 kg of wastewater and 400-600 kg of solid wastes characterized by a water content ranging between 25% and 50% (Azbar et al., 2004). For these reasons, the objective of this paper was to use this local BOP as secondary raw material in wastewater treatments, specifically for the retention of biopersistent pollutants as heavy metals. The present idea may represent a convenient, original and valid alternative in the environmental control operations, because a non-conventional sorbent may be also used for the removal of such toxic compounds as lead, cadmium and nichel ions. In fact, an incremental release of heavy metals in the environment has been the consequence of the increasing industrial use over the past decades (Femina Carolin et al., 2017, Azimi et al., 2017, Fu and Wang, 2011, Zhao et al., 2016, Shanmugam and Arabi

Mohammed Saleh, 2016). Leather tanning, mining and metal plating industries are among the main sources of e.g. lead, cadmium, copper, chromium, arsenic, zinc and nickel ions. Industrial effluents containing heavy metals represent a serious environmental problem due to the essential biopersistence of these pollutants leading to unacceptable sanitary risk and hazards in all natural compartments including man (Bánfalvi, 2011; Satyro et al., 2014).

In the present work, the retention properties of the BOP cellulosic biosorbent were evaluated in batch (equilibrium) and column (dynamic) tests. The Langmuir and Freundlich isotherms were used to correlate equilibrium data (Freundlich, 1906; Langmuir, 1918). Specifically, the sorbents were assumed to be used *"in once through operations"* to minimize problems related with the regeneration step, i.e., costs of regeneration chemicals, end disposal and fate of the hazardous spent regeneration eluates, etc.

After exhaustion, metals laden residues could be considered toxic, but the final aim of this paper was to propose the possible re-use the reference polluted secondary raw materials for applications in the building industry, specifically in lightweight cement conglomerates formula thus minimizing their potential impact to the environment (Petrella et al., 2016, 2012).

So, in summary, the objective of this study relies in the application of biosorbents from the agro-food industry for the removal of heavy metals from water and wastewater, with the final employment of the exhausted lignocellulosic material in the construction field.

2.Experimental section

2.1 BOP characterization

BOP for thermodynamic and kinetic tests was acquired from Rubino olive-oil manufacturing, Bari, Italy.

2 kg representative raw sample was initially dried and crushed, then sieved and pre-conditioned with 1 M HCl and 1 M NaOH solutions (three times) and thoroughly washed with demi water to

neutral pH. For practical problems in technological applications in the environmental area (i.e., removal of metals and release of noxious organics to the liquid-phase), it was necessary to clean-up BOP in such a way due to the presence of soluble organics (e.g., fulvic, humic acids, or other degradation products from natural degradation of the cellulosic backbone of BOP). The sorbent was successively air dried and finally put in the oven at 105°C. The dried material was crushed again in the range 1-3 mm before testing.

Elemental analysis was performed with Euro EA Elemental Analyser, Wegberg, Germany, the average BOP composition was 47% C, 2.7% N, 5.5% H, 44.8 O (Jain et al., 2013).

SEM morphology confirmed that BOP surface exhibits a linear groove structure with regular porous and fine fibers (Fig. 1). The samples were fixed on aluminium stubs with colloidal graphite and then sputtered with a 30 nm thick carbon film using an Edwards Auto 306 thermal evaporator. Back-scattered electron (BSE) images were obtained with a Zeiss scanning electron microscope (SEM) model EVO50XVP (Carl Zeiss Microscopy GmbH, Jena, Germany). SEM operating conditions: accelerating potential 15 kV; probe current 500 pA.

EDX analysis of metals laden BOP was obtained by an electron microscope FESEM-EDX Carl Zeiss Sigma 300 VP (Carl Zeiss Microscopy GmbH, Jena, Germany).

BET surface area and pore size of the sorbent were determined by adsorption-desorption N_2 isotherms at 77 K, by an Autosorb IQ Chemi TCD instrument (Quantachrome Instruments, Boynton Beach, FL, USA). The biosorbent was apparently a mesoporous material with pore diameters ranging 20-500 Å, average pore radius 15.649 Å and BET total surface area exceeding 0.324 m^2/g. Referring to the pores, the total volume and surface area were respectively 0.002 cm^3/g and 0.225 m^2/g.

Figure 1.

FTIR-ATR spectra of BOP (Fig. 2A) was recorded within the 600–4000cm^{-1} range using a Fourier Transform Infrared spectrometer 670-IR (Agilent Technologies Inc., Santa Clara, CA, USA), whose resolution was set to 4 cm^{-1}. Specifically, 32 scans were summed for each acquisition. The surface incidence of the main functional groups of BOP was clearly observed, under the experimental conditions (Akar et al., 2009). Bands were detected in the wavenumber region between 3600 and 2800 cm^{-1} and 800-1800 cm^{-1}. The vibration detected at 3313 cm^{-1} suggested the presence of hydroxyl and amino moieties (Mousa et al., 2009). The former could be ascribed to cellulose and hemicellulose molecules, better evidenced at 1032 cm^{-1} and 1162 cm^{-1}, the latter to amino acids and/or proteins (Rizzi et al., 2017). The incidence of amino and carboxyl groups was inferred observing the bands at 1540 cm^{-1} and 1630 cm^{-1}. As for the presence of phenols and polyphenols, vibration modes of CH_3, CH_2, C-H moieties along with the stretching of polyphenolic aromatic rings C-C were detected between 1100 and 1500 cm^{-1} (Omar and Abd El -Baset Attia, 2013). Not surprisingly, the presence of lignin was confirmed observing the bands at 2920 cm^{-1} and 2840 cm^{-1}, assigned to C-H stretching of methyl and methylene groups. Others signals were detected at 1318 cm^{-1} and 1241 cm^{-1} indicating the C-O vibrations of carboxylate groups and the stretching of esters, ethers or phenol groups (Paganelli et al., 2003).

TGA were performed using STA 449 F1 Jupiter, Netzsch, Selb, Germany. The sample was analyzed in the range 25-550°C at the heating speed of 3°C/min and in air atmosphere.

TG and DTG analyses were performed in order to unveil the FTIR-ATR findings. Results are reported in Figure 2B. The typical curve of solid fuels, having several weight losses, was obtained. As expected, as a first step the evaporation of the free moisture content was observed at around 100 °C followed by important weight losses in the temperature range between 200 to 400 °C and 410-500 °C. The temperatures of decomposition suggested the presence of hemicellulose, cellulose and lignin. Indeed, in excellent agreement with literature (Kabakci and Aydemir, 2013, Tawarah and Rababah, 2013, La Rubia Garcia et al., 2012) the hemicellulose/cellulose degradation occurs between 200 and 350 °C with maximum rate of degradation at 269°C as observed in the present

condition (if the hemicellulose degradation was exactly at 269°C, the cellulose decomposition occured at above 320 °C); the decomposition of lignin also occurs in this range of temperature and continued up to 600 °C (see inset Figure 2B, the peak at 333 °C).

Figure 2.

2.2 Sorption experiments. Batch (equilibrium) and column (dynamic) tests

Sorption experiments were carried out by the use of 1-3 mm BOP samples which were contacted with metals containing solutions representative of typical industrial wastewater. Synthetic solutions were prepared from reactive grade $Pb(NO_3)_2$, $Cd(NO_3)_2 \cdot 4H_2O$, $Ni(NO_3)_2 \cdot 7H_2O$ from Carlo Erba, Milan, Italy.

Batch equilibrium isotherms were correlated by Freundlich and Langmuir models. Application of Langmuir and Freundlich models is strictly dependent from the nature of the equilibrium data (Freundlich, 1906; Langmuir, 1918). The first model is conventionally applied for monolayer sorption when all the adsorption sites are equivalent and able to accommodate only one molecule:

$$q_{eq} = \frac{q_{max} b C_{eq}}{1 + b C_{eq}} \quad (1)$$

q_{eq} is the observed retention capacity onto the sorbent (mg/g); q_{max} is the maximum retention capacity (mg/g); b is an equilibrium constant; C_{eq} is the equilibrium concentration (mg/L).

Langmuir equation may be linearized to get the sorption constants:

$$\frac{C_{eq}}{q_{eq}} = \frac{1}{q_{max} b} + \frac{C_{eq}}{q_{max}} \quad (2)$$

Freundlich model, represented by the following empirical equation, assumes heterogenous surface:

$$q_{eq} = K_f C_{eq}^{1/n} \quad (3)$$

K_f is a constant related to the sorption capacity; n is related to the sorption intensity (energy) at the functional groups; C_{eq} is the equilibrium concentration (mg/L).

The Freundlich equation too may be rearranged to the linear form to get the relative constants:

$$lnq_{eq} = \frac{1}{n} lnC_{eq} + lnK_f$$

From the applicative point of view, in a first set of batch experiments, single metal containing solutions in demi-water (200 cm^3, 10 $mgMe^{+2}/L$, pH = 6) were contacted with known amounts of sorbent in the range of 2–400 mg. In a second set of batch experiments, ternary metal solutions in demi-water (200 cm^3, 10 mg Me^{+2}/L each, pH = 6) were contacted with the sorbent in the range of 5–600 mg. In a third set of batch experiments, ternary metal containing solutions in tap-water (200 cm^3, 0.3 mg Me^{+2}/L each, pH = 7.5) were contacted with the sorbent in the range of 1–100 mg. Equilibrations were carried-out in vials at 25°C by the use of a rotating stirrer (80 rpm) for one day, i.e., when the supernatant solution concentration changed by less than 5% after two subsequent samplings.

Laboratory column (dynamic) tests allowed for a deeper insight into the interactions of metals at the liquid-solid interface by the construction of the metals breakthrough curves. Breakthrough curves represent the variation of the relative effluent concentration (C/C_0) eluted by the column along time (t) or the effluent liquid volumes at constant flow-rate in the column (Bed Volumes, BV). The breakpoint corresponds to the minimum retention capacity of the sorbent toward metals packed into the column. Complete exhaustion of the biosorbent corresponds to equal concentrations of the effluent and influent solutions flowing through the column.

From an applicative point of view, column experiments were carried by the use of jacketed glass column (I.D. = 1.0 cm; H = 50 cm) packed with 5.5 g of BOP. Elution of the column was carried out with demi-water ternary metals solution (10 mg Me^{+2}/L each, pH = 6) at a flow-rate ranging 0.7 L/h. Each dynamic test was extended to complete column breakthrough, i.e., when the effluent from the column was equal to the influent solution concentration.

Liquid-phase metals concentrations, detected during batch and column experiments, were determined by Flame Atomic Absorption Spectrometry using a Mod. 929 Spectrometer from

Unicam, Milan, Italy. The technique is based on the principle that ground state metals absorb light at a specific wavelength and metal ions are converted to atomic state by a flame. After absorption of a specific wavelength, the amount absorbed is measured and a concentration is obtained.

Table 1 summarizes the complex of laboratory tests carried out.

Table 1.

2.3 Metals leaching test from BOP containing mortars and thermo-mechanical measurements

After exhaustion, heavy metals laden BOP were embedded into cement mortars as replacement of the conventional aggregates. Class II CEM A-LL, 42.5R cement, from Buzzi Unicem, Barletta, Italy (Italian Organization for Standardization, 2011), was used to prepare the conglomerates. 400 cm^3 BOP was added according to standard protocols (Italian Organization for Standardization, 2016), cube samples (4×4×4 cm) were prepared and aged for 28 days at relative humidity, RH >90%, then dried to constant weight. Specimens were submitted to jar test (Vittadini, Aqua, Milan, Italy) to evaluate potential release of Pb^{2+}, Cd^{2+}, and Ni^{2+} species, which was carried out after filtration and analysis of the supernatant solution (Italian Organization for Standardization, 2002).

Thermal measurements were carried-out on cylinder specimens (φ = 100 mm; H = 50 mm) by a Mod. ISOMET 2104 system, from Applied Precision Ltd (Bratislava, Slovakia), after 28 days curing. Thermal conductivity was determined after placing a heating probe on the front face of the sample thus geerating a constant thermal flow. A normalized mortar was prepared as control.

Mechanical tests (compression) were carried out by a MATEST system, Milan, Italy, on samples deriving from mechanical flexural tests. Specifically, prisms (40×40×160 mm) were prepared according to standard protocols (Italian Organization for Standardization, 2016) and 28 days cured, while normalized mortar was prepared as control.

3. Results and discussion

Figure 3A and 3B show batch (equilibrium) curves for single ions metal retention at constant concentration (10 mg/L, 25°C). Freundlich and Langmuir correlations are shown in Figures 3C and 3D. Equilibrations were carried-out in de-mineralized water, pH = 6, which was considered the optimum for experimental tests because, as reported elsewhere (Doyurum and Çelik, 2006; El-Kady et al., 2016; Fiol et al., 2006; Saeed et al., 2005), sorption for all metals at low pH, i.e., 2-4 was shown to be negligible, with best results in the range of 5-6. Specifically, negatively charged groups at the biosorbent surface are necessary for metals sorption, whereas acidic pH, i.e. 2, limits interactions as a net positive charge on the biosorbent is formed after protonation reaction, thus competing with metals at the active sites. At higher pH, a negatively charged surface is formed onto the biosorbent surface thus favouring metal uptake. Further pH increase induces metals precipitation (Doyurum and Çelik, 2006; El-Kady et al., 2016; Fiol et al., 2006; Saeed et al., 2005).
It was observed that, with the increase of the sorbent dosage, the maximum sorbed quantities ($mgMe^{2+}/g$) decreased (Figure 3A) and the metals removal increased (Figure 3B) (Dakiky et al., 2002; Pradhan et al., 1999; Rengaraj et al., 2001). Moreover, almost 100% of every metal retention was obtained as reported in Figure 3B. Table 2 summarizes the experimental maximum retentions.

Figure 3.

Table 2.

Maximum retention capacities were determined, for Pb, Cd and Ni respectively, at 22.4; 10.5 and 5.04 $mg/g_{sorbent}$. A relevant role in determining the overall metals retention capacities is played by the BOP specific surface area and the corresponding larger sorbent pores (Figure 1) exposed to the liquid-phase, together with metals hydrated radius. Free migration of metal ions to the functional

253 groups of the biosorbent was allowed by the large openings (porosity) in the cellulosic matrix
254 (Manliu et al., 1994). Accordingly, the free energies of hydration/de-hydration of the metal ions
255 should play a more important role in determining the overall interaction onto the biosorbent surface
256 (Robinson and Stokes, 1970). The lowest interaction energy (electrostatic) and hydration radius
257 (hindrance) (Table 3) confirm that lead ions were preferentially sorbed as compared to the largest
258 radius and higher free energy of cadmium ions (Robinson and Stokes, 1970). Indeed, lead ions
259 showed higher retention capacity as compared to cadmium ions because of the most favorable
260 compromise between permeation (smaller hydrated radius) and interaction (easier ionic dehydration
261 at functional groups). Lead ions also showed higher retention capacity as compared to nickel ions;
262 in this case the interaction seems to be preferentially associated with dehydration energy because
263 both ions show almost the same ionic radius. Cadmium ions showed higher retention capacity as
264 compared to nickel ions; in this case electrostatic factors play a more relevant role than steric
265 hindrance.
266
267
268 Table 3.
269
270 Moreover, Table 2 shows the relevant models parameters derived from Figures 3C and 3D.
271 Specifically, various direct parameters calculated from the adsorption isotherms, namely, maximum
272 retention capacity (q_{max}), adsorption efficiency (b) and confidence parameter (R^2) from the
273 Langmuir isotherms, and derived sorption capacity of the sorbent (K_f), sorption intensity (1/n) and
274 confidence parameter (R^2) from the Freundlich isotherms are shown. The confidence parameters
275 indicate that both models can be applied for data correlation.
276 Nonetheless, the separation factor R_L is a characteristic of the Langmuir model and can be
277 calculated from the following equation (Hall et al., 1966): $R_L = 1/(1+bC_0)$ where C_0 is the initial
278 concentration of the adsorbate (mg/L) and b (L/mg) is the Langmuir constant. R_L is related to the

shape of the isotherm, e.g., unfavorable retention, $R_L > 1$; indifferent equilibrium, $R_L = 1$; favorable equilibrium, $0 < R_L < 1$; irreversible equilibrium, $R_L = 0$ (Hameed et al., 2009). R_L values for the metals adsorption on BOP were in the range 0-1, which means favorable retention toward species of interest.

Table 4 shows a comparison with the retention capacities obtained by other authors. Specifically, similar results can be observed in the case of raw materials, although metal sorption figures tend to increase in the case of chemical treatments of the biomass. In the latter case, the modification techniques are employed to enhance and reinforce the functional groups potential and increase the number of active sites.

Table 4.

In ternary demi water solutions a definite preference of the biosorbent toward lead ions was also evidenced (Figures 4A and B) (Saeed et al., 2005) with a selectivity scale in the following order: $Pb^{++} > Cd^{++} > Ni^{++}$. As discussed before (single ion solutions), lead ions showed the best performance because of the lowest interaction energy and hydration radius as compared to cadmium and nichel ions. Moreover, at higher sorbent dosage maximum sorbed quantities ($mgMe^{2+}/g$) decreased (Figure 4A), metals removal increased and almost 100% of every metal retention was obtained (Figure 4B) (Dakiky et al., 2002; Pradhan et al., 1999; Rengaraj et al., 2001). Generally speaking, experimental q_{max} exceeding 10.51, 5.11 and 3.81 $mg/g_{sorbent}$, respectively for Pb, Cd and Ni, were observed (Table 5), definitely lower figures as compared to single ion solutions. Reduction in the retention capacities in the case ternary solutions may be attributed to the greater cumulative occupancy by the larger ions at the BOP surface. Freundlich and Langmuir correlations are shown in Figures 4C and 4D, while Table 5 also shows the relevant models parameters. Both models can be applied for data correlation and no significant differences were observed between single and

304 ternary systems. Also in this case the value of R_L of the Langmuir model indicates a favorable
305 process for the adsorption of the metals on BOP.
306
307 Figure 4.
308 Table 5.
309
310 In the case of measurements in tap water solutions, the presence of major divalent and monovalent
311 ions, i.e., Ca^{2+}, Mg^{2+}, Na^{+}, etc, determined a large decrease of the retentions (Figures 5A and 5B).
312 Generally speaking, experimental q_{max} exceeding 1.20, 0.80 and 0.74 $mgMe^{2+}/g_{sorbent}$, respectively
313 for Pb^{+2}, Cd^{+2}, and Ni^{+2} were observed (Table 6). On the other hand, potential formation of
314 negatively charged metal complexes with anions (chlorides) may lead to Donnan exclusion thus
315 further reducing the biosorbent performance (Helfferich, 1962). Freundlich and Langmuir
316 correlations are shown in Figures 5C and 5D, while Table 6 also shows the relevant models
317 parameters.
318 It is known that main peculiarities of the Freundlich and the Langmuir models are the assumption
319 that the first forms a multilayer, the second forms a monolayer of the sorbed species. In this context,
320 experimental data for tests carried-out in demineralized water were pretty well correlated by both
321 models. In the case of the experiments carried-out in tap water, correlations based on the Freundlich
322 model were definitely better than the other. This may be supposedly explained in terms of sorbate
323 multilayer formation. In the case of tap water, the massive presence of alternative ions (calcium and
324 magnesium) may preferentially saturate the first layer thus leaving to the minor metal species of
325 interest almost no room for the interaction at the sorbent active groups. This may explain the poor
326 correlation of the Langmuir model.
327
328 Figure 5.

Table 6

Column (dynamic) tests were carried-out for a deeper insight into the interactions of the metals at the liquid-solid interface by the construction of the breakthrough curves. Operations were obtained in stationary conditions by the elution of ternary metals solutions (C= 10 $mgMe^{2+}/L$ each in demi-water) at constant flow-rate in the column exceeding 0.7 L/h. Fig.6A and B show the experimental breakthrough curves (Petrella et al., 2012, 2010).

Figure 6.

Relevant data at metals breaktrough are shown in Table 7. Results from the column tests confirmed thermodynamic data. Also in this case a definite preference of the biosorbent toward lead ions was evidenced with a selectivity scale in the following order:

$$Pb^{++} > Cd^{++} > Ni^{++}$$

corresponding to an anticipated breakthrough point in the case of less sorbed metals occurring at lower effluent Bed Volumes (V/V_0). The overall operating capacities for different metals, at complete column breakthrough, resulted to be also in the same order:

$$q_{Pb}{}^{++} > q_{Cd}{}^{++} > q_{Ni}{}^{++}$$

quantitatively identified in 5.33 $mgPb^{++}/g_{BOP}$; 2.71 $mgCd^{++}/g_{BOP}$; and 1.98 $mgNi^{++}/g_{BOP}$ respectively, as summarized in Table 7.

Table 7.

From the applicative point of view, in batch (equilibrium) and column (dynamic) operations the sorbents were used *"in once through operations"* to minimize technical and economic problems related with the regeneration step.

For this reason, after retention, metals exhausted materials were finally used (disposed) in cement mortars formula as replacement of conventional aggregates thus minimizing their potential impact to the environment (Petrella et al., 2016, 2012, 2009). To the purpose, in order to evaluate possible release of lead, cadmium and nichel ions, mortar specimens including metals laden biosorbents were submitted to jar test (Italian Organization for Standardization, 2002). It was observed (Table 8) that the release of metals to the liquid-phase was below the maximum allowable concentrations for hazardous waste disposal in controlled landfills.

Table 8.

Moreover, EDX observation for the metal laden BOP showed no particular changes on the structure of the biosorbent and, after semi-quantitative analysis of the heavy metals retained by the solid phase, it was observed that the wt% ratios between the metal species were very comparable with the ratios between the overall capacities (Fig. 7).

Figure 7.

After jar test, which demonstrated negligible release of metals, the specimens were characterized for possible applications in the construction field. The preliminary results of the metal laden composites suggest that the specimens show very low thermal conductivities λ (0.18 W/mK) as opposite to the conventional sand based control (2.0 W/mK) but the mechanical properties are quite low (~1 N/mm^2) which suggests to introduce in the metals laden mortar other metal laden

aggregates (recycled porous glass, studied in previous works (Petrella et al., 2012) which can increase compressive resistances.

Basically, the application of these conglomerates may be as non structural thermo-insulating and lightweight materials in the construction industry (panels, plasters) due to the presence of a metal laden waste as the lignocellulosic aggregates.

Conclusions

The objective of this paper was based on the application of biosorbents from the olive oil milling operations (BOP from South-East Italy) for the removal of lead, cadmium and nichel ions present in water and wastewater, with final possible re-use of the metals laden materials in the construction field.

Specifically, the sorption properties of the reference wastes toward metal ions was demonstrated through batch (equilibrium) and column (dynamic) tests.

In the present case, no preliminary treatments were carried-out on the sorbents to improve the retention capacities.

From batch tests, maximum metals retentions in single ion solutions were 22.4 mg/g_{BOP}, 10.5 mg/g_{BOP}, 5.04 mg/g_{BOP} respectively for Pb^{+2}, Cd^{+2} and Ni^{+2}, while in the case of ternary systems, maximum metals retentions were 10.51 mg/g_{BOP}, 5.11 mg/g_{BOP}, 3.81 mg/g_{BOP} respectively for Pb^{+2}, Cd^{+2} and Ni^{+2}.

Best retention toward lead ion was attibuted to the hydrated radius and free energies of hydration/de-hydration of the metal ions.

Reduction in the retention capacities in the case of ternary solutions respect to single ion solutions may be attributed to the greater cumulative occupancy by the larger ions at the BOP surface.

The lowest retentions were detected in tap water due to the presence of major divalent and monovalent ions and to the potential formation of negatively charged metal complexes with anions (chlorides) leading to Donnan exclusion.

Langmuir and Freudlich isotherms gave a good correlation of the experimental data in single-ion and ternary solutions, while the Freundlich model resulted better in tap-water solutions.

Also in the case of the column (dynamic) tests a definite preference of the biosorbent toward lead ions was evidenced with the following retentions: 5.33 $mgPb^{++}/g_{BOP}$; 2.71 $mgCd^{++}/g_{BOP}$; and 1.98 $mgNi^{++}/g_{BOP}$.

Final destination of metals laden BOP wastes was the inclusion into lightweight cement mortars formula as a quantitative substitution of the conventional aggregates in consideration of the minimized potential release of metals detected after the water leaching tests carried-out on the consolidated specimens.

Moreover, low thermal conductivities λ (0.18 W/mK) of the prepared cement composites were observed as opposite to the conventional sand based control (2.0 W/mK) but the mechanical properties were quite low (~1 N/mm^2) thus suggesting to introduce in the metals laden mortar other more resistant aggregates in order to employ these conglomerates for non structural lightweight applications (panels, plasters).

Acknowledgments

The authors wish to thank Prof. Giuseppe Romanazzi, for elemental analysis. The authors also thank Mr. Adriano Boghetich for SEM-EDX analysis and Prof. Pietro Stefanizzi for thermal measurements. Regione Puglia is gratefully acknowledged for financial support (X-Ray Lab Project–Reti di Laboratori Pubblici di Ricerca, cod. n. 45 and 56).

References

Abdolali, A., Guo, W.S., Ngo, H.H., Chen, S.S., Nguyen, N.C., Tung, K.L, 2014. Typical lignocellulosic wastes and by-products for biosorption process in water and wastewater treatment: A critical review. Bioresour. Technol. 160, 57–66.

Ahmad, A., Khatoon, A., Mohd-Setapar, S.-H., Kumar, R., Rafatullah, M., 2016. Chemically oxidized pineapple fruit peel for the biosorption of heavy metals from aqueous solutions. Desalin. Water Treat. 57(14), 6432-6442.

Ahmad, N., Hussain, T., Nasir Awan, A., Sattar, A., Arslan, C., Qamar Tusief, M., Mariam, Z., 2017. Efficient and eco-friendly management of biodegradable municipal solid waste (MSW) using naturally aerated windrow composting technique in District Lahore Pakistan. Earth Science Pakistan, 1(1), 1-4.

Ashraf, M.A., Hussin, N.H., Gharibreza, M., 2017. Studies on the removal of heavy metals from aqueous solution using immobilized Typha angustata L. Earth Science Pakistan, 1(1), 11-14.

Akar, T., Tosun, I., Kaynak, Z., Ozkara, E., Yeni, O., Sahin, E.N., Tunali Akar, S., 2009. An attractive agro-industrial by-product in environmental cleanup: dye biosorption potential of untreated olive pomace. J. Hazard. Mater. 166, 1217-1225.

Alslaibi, T. M., Abustan, I., Ahmad, M. A., Foul, A. A., 2013. Cadmium removal from aqueous solution using microwaved olive stone activated carbon. J. Environ. Chem. Eng. 1 (3), 589–599.

Alslaibi, T. M., Abustan, I., Ahmad, M.A., Abu Foul, A., 2014. Kinetics and equilibrium adsorption of iron (II), lead (II), and copper (II) onto activated carbon prepared from olive stone waste. Desalin. Water Treat. 52, 40-42, 7887-7897.

Alslaibi, T. M., Abustan, I., Ahmad, M.A., Abu Foul, A., 2014. Preparation of Activated Carbon From Olive Stone Waste: Optimization Study on the Removal of Cu^{2+}, Cd^{2+}, Ni^{2+}, Pb^{2+}, Fe^{2+}, and Zn^{2+} from Aqueous Solution Using Response Surface Methodology. J. Disper. Sci. Technol., 35, 7, 913-915.

Al-Anber, Z.A., Matouq, M.A.D., 2008. Batch adsorption of cadmium ions from aqueous solution by means of olive cake. J. Hazard. Mater. 151, 194–201.

Anastopoulos, I., Panagiotou, M., Ehaliotis, C., Tarantilis, P. A., Massas, I., 2015. NaOH pretreatment of compost derived from olive tree pruning waste biomass greatly improves biosorbent characteristics for the removal of Pb^{2+} and $Ni^{2+}$from aqueous solutions. Chem. Ecol. 31, 8, 724-740.

Anwar, J., Shafique, U., Waheed uz, Z., Salman, M., Dar, A., Anwar, S., 2010. Removal of Pb(II) and Cd(II) from water by adsorption on peels of banana. Bioresour. Technol. 101, 1752–1755.

Azbar, N., Bayram, A., Filibeli, A., Muezzinoglu, A., Sengul, F., Ozer, A., 2004. A Review of Waste Management Options in Olive Oil Production. Crit. Rev. Env. Sci. Tec. 34, 209–247.

Azimi, A., Azari, A., Rezakazemi, M., Ansarpour, M., 2017. Removal of Heavy Metals from Industrial Wastewaters: A Review. Chem Bio Eng Rev. 4, 1, 1-24.

Baccar, R., Bouzid, J., Feki, M., Montiel, A., 2009. Preparation of activated carbon from Tunisian olive-waste cakes and its application for adsorption of heavy metal ions. J. Hazard. Mater. 162(2-3), 1522-1529.

Bánfalvi, G., 2011. Cellular Effects of Heavy Metals, Springer, New York.

Bhatnagar, A., Minocha, A.K., 2010. Biosorption optimization of nickel removal from water using Punica granatum peel waste. Colloid Surface B. 76, 544–548.

Blázquez, G., Martín-Lara, M.A., Tenorio, G., Calero, M., 2011. Batch biosorption of lead(II) from aqueous solutions by olive tree pruning waste: Equilibrium, kinetics and thermodynamic study. Chem. Eng. J. 168(1), 170-177.

Bohli, T., Ouederni, A., Fiol, N., Villaescusa, I., 2015. Evaluation of an activated carbon from olive stones used as an adsorbent for heavy metal removal from aqueous phases. C.R. Chim. 18 (1), 88–99.

Calero, M., Pérez, A., Blázquez, G., Ronda, A., Martín-Lara, M.A., 2013. Characterization of chemically modified biosorbents from olive tree pruning for the biosorption of lead. Ecol. Eng. 58, 344–354.

508 Calero, M., Ronda, A., Martin-Lara, M.A., Perez, A., Blazquez, G., 2013. Chemical activation of
509 olive tree pruning to remove lead(II) in batch system: Factorial design for process optimization.
510 Biomass Bioenerg. 58, 322-332.
511 Chao, H.P., Chang, C.C., 2012. Adsorption of copper (II), cadmium (II) and lead (II) from aqueous
512 solution using biosorbent. Adsorption. 18, 395-401.
513 Chiarantini, L., Rimondi, V., Benvenuti, M., Beutel, M.W., Costagliola, P., Gonnelli, C., Lattanzi,
514 P., Paolieri, M., 2016. Black pine (Pinus nigra) barks as biomonitors of airborne mercury
515 pollution. Sci. Total Environ. 569-570, 105-113.
516 Chouchene, A., Jeguirim, M., Trouve, G., 2014. Biosorption performance, combustion behavior,
517 and leaching characteristics of olive solid waste during the removal of copper and nickel from
518 aqueous solutions. Clean Technol. Environ. Policy 16(5), 979-986.
519 Çifçi, D.I., Meriç, S., 2016. A review on pumice for water and wastewater treatment. Desalin.
520 Water Treat. 57 (39), 18131-18143.
521 Dakiky, M., Khamis, M., Manassra, A., Mer'eb, M., 2002. Selective adsorption of chromium(VI) in
522 industrial wastewater using low-cost abundantly available adsorbents. Adv. Environ. Res. 6(4),
523 533–540.
524 do Nascimento, G.E., Campos, N.F., da Silva, J.J., Barbosa, C.M.B.D.M., Duarte, M.M.M.B.,
525 2016. Adsorption of anionic dyes from an aqueous solution by banana peel and green coconut
526 mesocarp. Desalin. Water Treat. 57(30), 14093-14108.
527 Doyurum, S., Çelik, A., 2006. Pb(II) and Cd(II) removal from aqueous solutions by olive cake. J.
528 Hazard. Mater. 138(1), 22-28.
529 El-Kady, A.A., Carleer, R., Yperman, J., D'Haen, J., Abdel Ghafar, H.H., 2016. Kinetic and
530 adsorption study of Pb (II) toward different treated activated carbons derived from
531 olive cake wastes. Desalin. Water Treat. 57(18), 8561-8574.

532 Femina Carolin, C., Senthil Kumar, P., Saravanan, A., Janet Joshiba, G., Naushad, Mu., 2017.
533 Efficient techniques for the removal of toxic heavy metals from aquatic environment: a Review. J.
534 Environ. Chem. Eng., 5, 3, 2782-2799.
535 Fernández-Pereira, C., De La Casa, J.A., Gómez-Barea, A., Arroyo, F., Leiva, C., Luna, Y., 2011.
536 Application of biomass gasification fly ash for brick manufacturing. Fuel 90(1), 220-232.
537 Fiol, N., Villaescusa, I., Martínez, M., Miralles, N., Poch, J., Serarols, J., 2006. Sorption of Pb(II),
538 Ni(II), Cu(II) and Cd(II) from aqueous solution by olive stone waste. Sep. Purif. Technol. 50(1),
539 132-140.
540 Fomina, M., Gadd, G.M., 2014. Biosorption: Current perspectives on concept, definition and
541 application. Bioresour. Technol. 160, 3–14.
542 Freundlich, H.M.F., 1906. Uber die adsorption in losungen. Z. Phys. Chem. 57, 385-470.
543 Fu, F., Wang, Q., 2011. Removal of heavy metal ions from wastewaters: A review. J. Environ.
544 Manage. 92(3), 407-418.
545 Guo, X.Y., Liang, S., Tian, Q.H., 2011. Removal of heavy metal ions from aqueous solutions by
546 adsorption using modified orange peel as adsorbent. Adv. Mater. Res. 236–238, 237–240.
547 Hall, K.R., Eagleton, L.C., Acrivos, A., Vermeulen, T., 1966. Pore-and solid-diffusion kinetics in
548 fixed-bed adsorption under constant-pattern conditions. Ind. Eng. Chem. Fundam. 5(2), 212–223.
549 Hameed, B.H., Salman, J.M., Ahmad, A.L., 2009. Adsorption isotherm and kinetic modeling of 2,4-
550 D pesticide on activated carbon derived from date stones. J. Hazard. Mater. 163(1), 121–126.
551 Hawari, A., Khraisheh, M., Al-Ghouti, M. A., 2014. Characteristics of olive mill solid residue and
552 its application in remediation of Pb^{2+}, Cu^{2+} and Ni^{2+} from aqueous solution: Mechanistic study
553 Chem. Eng. J. 251, 329-336.
554 Helfferich, F., 1962. Ion exchange, McGraw Hill, New York.
555 Hossain, M.A., Ngo, H.H., Guo, W.S., Setiadi, T., 2012. Adsorption and desorption of copper(II)
556 ions onto garden grass. Bioresour. Technol. 121, 386–395.

557 Ismail, T.H.T., Adnan, N.A.F., Samah, M. A. A., 2017. The accumulation of Fe, Pb, Zn, Ni and Cd
558 in Nerita lineata and Thais bitubercularis obtained from Tanjung Harapan and Teluk Kemang,
559 Malaysia, J. Clean WAS, 1(1), 6-16.
560 Italian Organization for Standardization (UNI). Cement Composition, Specifications and
561 Conformity Criteria for Common Cements. EN 197-1. Available online:
562 http://store.uni.com/magento-1.4.0.1/index.php/en-197-1-2011.html (accessed on 14-09-2011).
563 Italian Organization for Standardization (UNI), Methods of Testing Cement-Part 1: Determination
564 of Strength. EN 196-1. Available online: http://store.uni.com/magento-1.4.0.1/index.php/en-196-1-
565 2016.html (accessed on 27-04-2016).
566 Italian Organization for Standardization (UNI), Characterization of Waste-Compliance Test for
567 Leaching of Granular Waste Materials and Sludges. EN 12457-2. Available online:
568 http://store.uni.com/magento-1.4.0.1/index.php/en-12457-2-2002.html (accessed on 18-09-2002).
569 Jafar Ahamed, A., Loganathan, K., 2017. Water quality concern in the Amaravathi River Basin of
570 Karur district: a view at heavy metal concentration and their interrelationships using geostatistical
571 and multivariate analysis. Geology, Ecology, and Landscapes, 1(1), 19-36.
572 Jain, M., Garg, V.K., Kadirvelu, K., 2013. Cadmium(II) sorption and desorption in a fixed bed
573 column using sunflower waste carbon calcium-alginate beads. Bioresour. Technol. 139, 242–248.
574 Kabakci, S.B., Aydemir, H., 2013. Pyrolysis of olive pomace and copyrolysis of olive pomace with
575 refuse derived fuel. Environ Prog Sustain Energy, 33, 649-56
576 Khan, A., Rehman, R., Rashid, H., Nasir, A., 2017, Exploration of environmental friendly
577 adsorbents for treatment of azo dyes from textile wastewater and its dosage optimization. Earth
578 Science Pakistan, 1(1), 5-7.
579 Konstantinou, M., Kolokassidou, K., Pashalidis, I., 2007. Sorption of Cu(II) and Eu(III) ions from
580 aqueous solution by olive cake. Adsorption 13(1), 33-40.

581 Kumar, P.S., Ramalingam, S., Kirupha, S.D., Murugesan, A., Vidhyadevi, T., Sivanesan, S., 2011.
582 Adsorption behavior of nickel(II) onto cashew nut shell: equilibrium, thermodynamics, kinetics,
583 mechanism and process design. Chem. Eng. J. 167, 122–131.
584 La Rubia-García, M.D., Yebra-Rodríguez, A., Eliche-Quesada, D., Corpas-Iglesias, F.A., Lopez-
585 Galindo, A., 2012. Assessment of olive mill solid residue (pomace) as an additive in lightweight
586 brick production. Con Buil Mat. 36, 495-500.
587 Langmuir, I., 1918. The adsorption of gases on plane surface of glass, mica and platinum. J. Am.
588 Chem. Soc. 40, 1361-1403.
589 Manliu, E., Loizidou, M., Spyrellis, N., 1994. Uptake of lead and cadmium by clinoptilolite. Sci.
590 Total Environ. 149, 139–144.
591 Martín-Lara, M.A., Hernáinz, F., Calero, M., Blázquez, G., Tenorio, G., 2009. Surface chemistry
592 evaluation of some solid wastes from olive-oil industry used for lead removal from aqueous
593 solutions. Biochem. Eng. J. 44(2-3), 151-159.
594 Martín-Lara, M. A., Blazquez, G., Ronda, A., Perez, A., Calero, M., 2013. Development and
595 characterization of biosorbents To remove heavy metals from aqueous solutions by chemical
596 treatment of olive stone. Ind. Eng. Chem. Res. 52, 10809-10819.
597 Michalak, I., Chojnacka, K., Witek-Krowiak, A., 2013. State of the art for the biosorption process.
598 A review. Appl Biochem Biotechnol. 170(6), 1389–1416.
599 Mosa, A., El-Ghamry, A., Trüby, P., Omar, M., Gao, B., Elnaggar, A., Li, Y., 2016. Chemo-
600 mechanical modification of cottonwood for Pb^{2+} removal from aqueous solutions: Sorption
601 mechanisms and potential application as biofilter in drip-irrigation**.** Chemosphere. 161, 1-9.
602 Mousa, A., Heinrich, G., Gohs, U., Hassler, R., Wagenknecht, U., 2009. Application of renewable
603 agro-waste-based olive pomace on the mechanical and thermal performance of toughened PVC.
604 Polym-Plast Technol Eng. 48, 1030-1040.
605 Omar, HA, Abd El -Baset Attia, L., 2013. Kinetic and equilibrium studies of cesium-137 adsorption
606 on olive waste from aqueous solutions. Radiochemistry. 55, 497-504.

607 Pagnanelli, F., Mainelli, S., Vegliò,. F, Toro, L., 2003. Heavy metal removal by olive pomace:
608 biosorbent characterization and equilibrium modelling. Chem Eng Sci. 58, 4709-17.
609 Pei, Y.Y., Liu, J.Y., 2011. Adsorption of Pb^{2+} in wastewater using adsorbent derived from
610 grapefruit peel. Adv. Mater. Res. 391–392, 968–972.
611 Petrella, A., Petruzzelli, V., Ranieri, E., Catalucci, V., Petruzzelli, D., 2016. Sorption of Pb(II),
612 Cd(II) and Ni(II) from single- and multimetal solutions by recycled waste porous glass. Chem. Eng.
613 Commun. 203(7), 940-947.
614 Petrella, A., Petrella, M., Boghetich, G., Basile, T., Petruzzelli, V., Petruzzelli, D., 2012. Heavy
615 metals retention on recycled waste glass from solid wastes sorting operations: A comparative study
616 among different metal species. Ind. Eng. Chem. Res. 51(1), 119-125
617 Petrella, A., Petruzzelli, V., Basile, T., Petrella, M., Boghetich, G., Petruzzelli, D., 2010. Recycled
618 porous glass from municipal/industrial solid wastes sorting operations as a lead ion sorbent from
619 wastewaters. React. Funct. Polym. 70, 203–209.
620 Petrella, A., Petrella, M., Boghetich, G., Petruzzelli, D., Ayr, U., Stefanizzi, P., Calabrese, D., Pace,
621 L., 2009. Thermo-acoustic properties of cement-waste-glass mortars. Proc. Inst. Civ. Eng.: Constr.
622 Mater. 162(CM2), 67–72.
623 Pradhan, J., Das, S.N., Thakur, R.S., 1999. Adsorption of hexavalent chromium from aqueous
624 solution by using activated red mud. J. Colloid Interface Sci. 217, 137–141.
625 Qi, Y., Zhu, J., Fu, Q., Hu, H., Huang, Q., Violante, A., 2016. Sorption of Cu by organic matter
626 from the decomposition of rice straw. J. Soils Sediments 16(9), 2203-2210.
627 Ramalbo, R.S., 1977. Introduction to wastewater treatment process, Academic Press Inc., New
628 York.
629 Rengaraj, S., Kyeong-Ho, Y., Seung-Hyeon, M., 2001. Removal of chromium from water and
630 wastewater by ion exchange resins. J. Hazard. Mater. B 87, 273–287.

631 Rezania, S., Taib, S.M., Md Din, M.F., Dahalan, F.A., Kamyab, H., 2016. Comprehensive review
632 on phytotechnology: Heavy metals removal by diverse aquatic plants species from wastewater. J.
633 Hazard. Mater. 318, 587-599.
634 Rizzi, V., D'Agostino, F., Fini, P., Semeraro, P., Cosma, P., 2017. An interesting environmental
635 friendly cleanup: The excellent potential of olive pomace for disperse blue adsorption/desorption
636 from wastewater. Dyes Pigm. 140, 480-490.
637 Robinson, R.A., Stokes, R.H., 1970. Electrolyte Solutions, Courier Dover Publications, U.K.
638 Ronda, A., Martín-Lara, M.A., Calero, M., Blázquez, G., 2013. Analysis of the kinetics of lead
639 biosorption using native and chemically treated olive tree pruning. Ecol. Eng. 58, 278-285.
640 Saeed, A., Iqbal, M., Akhtar, M.W., 2005. Removal and recovery of lead(II) from single and
641 multimetal (Cd, Cu, Ni, Zn) solutions by crop milling waste (black gram husk). J. Hazard. Mater.
642 117(1), 65-73.
643 Satyro, S., Race, M., Marotta, R., Dezotti, M., Spasiano, D., Mancini, G., Fabbricino, M., 2014.
644 Simulated solar photocatalytic processes for the simultaneous removal of EDDS, Cu(II), Fe(III) and
645 Zn(II) in synthetic and real contaminated soil washing solutions. J. Environ. Chem. Eng. 2(4),
646 1969-1979.
647 Shanmugam, S., Arabi Mohammed Saleh, M.A., 2016. An overview of research trends in
648 remediation of heavy metal ion from polluted water. Int. J. Pharm.Tech Res. 9, 1, 90-96.
649 Tawarah, M.K., Rababah, R.A., 2013. Characterization of some Jordanian crude and exhausted
650 olive pomace samples. Green Sustain. Chem., 3, 146-62.
651 Velazquez-Jimenez, L.H., Pavlick, A., Rangel-Mendez, J.R., 2013. Chemical characterization of
652 raw and treated agave bagasse and its potential as adsorbent of metal cations from water. Ind. Crop.
653 Prod. 43, 200–206.
654 Zhao, M., Xu, Y., Zhang, C., Rong, H., Zeng, G., 2016. New trends in removing heavy metals from
655 wastewater. Appl. Microbiol. Biot. 100, 15, 6509-6518.

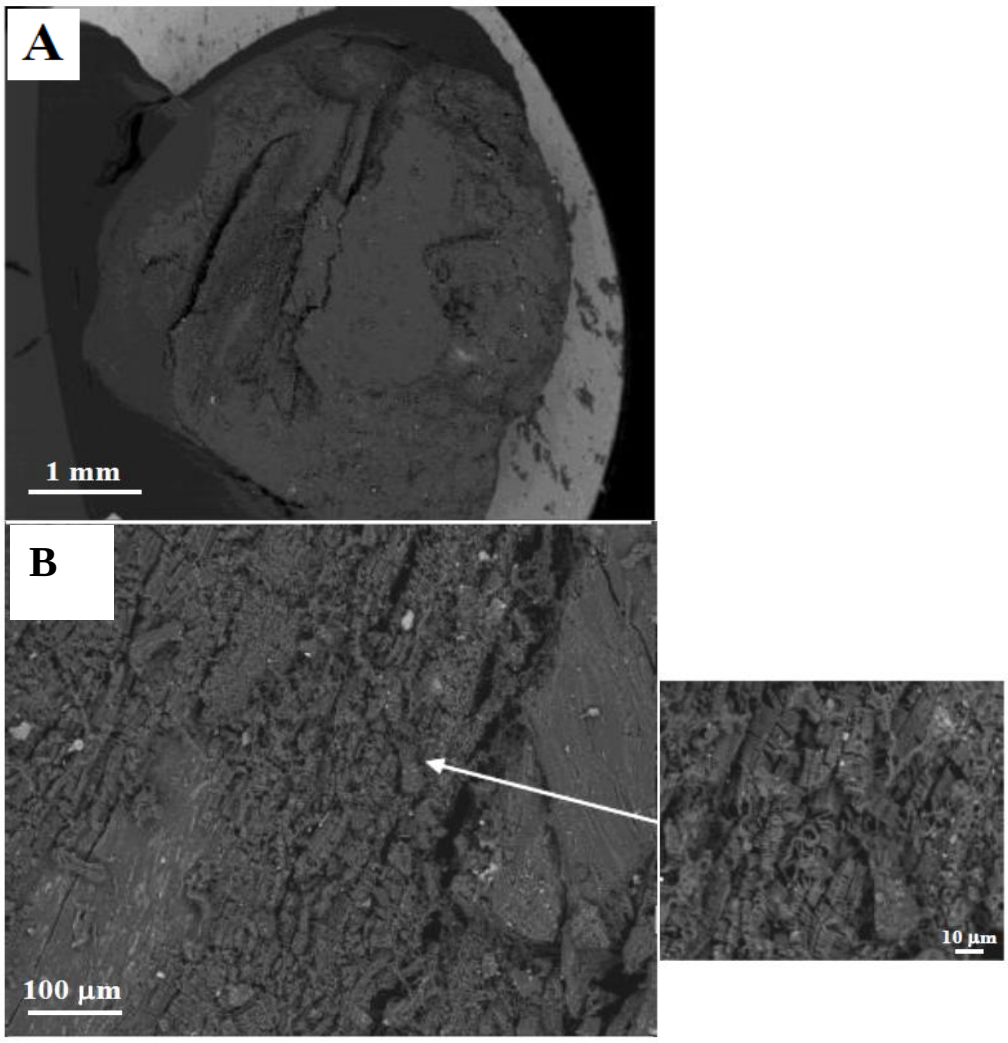

Figure 1. A) SEM back scattered electron images of a single BOP grain; B) BOP texture with the corresponding magnification. The white grains are silicate minerals, mainly feldspars and less frequent clay minerals.

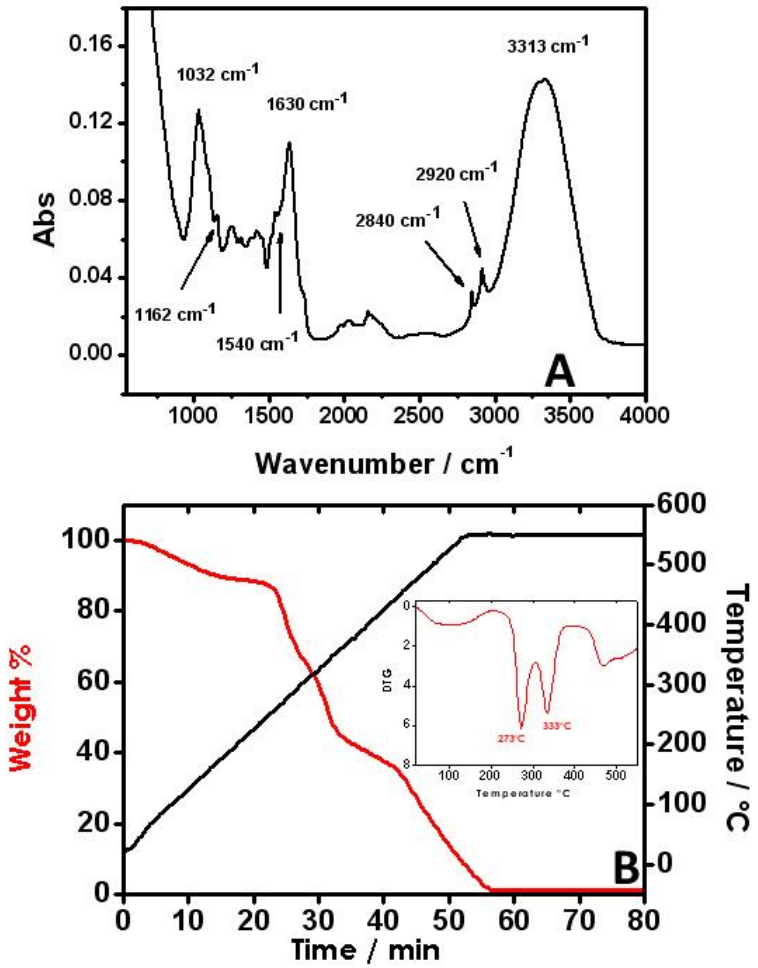

Figure 2. A) BOP FTIR–ATR spectra in the range 600-4000 cm^{-1}, B) Thermogravimetric (TG) and (inset) Differential Thermogravimetric (DTG) analyses of BOP.

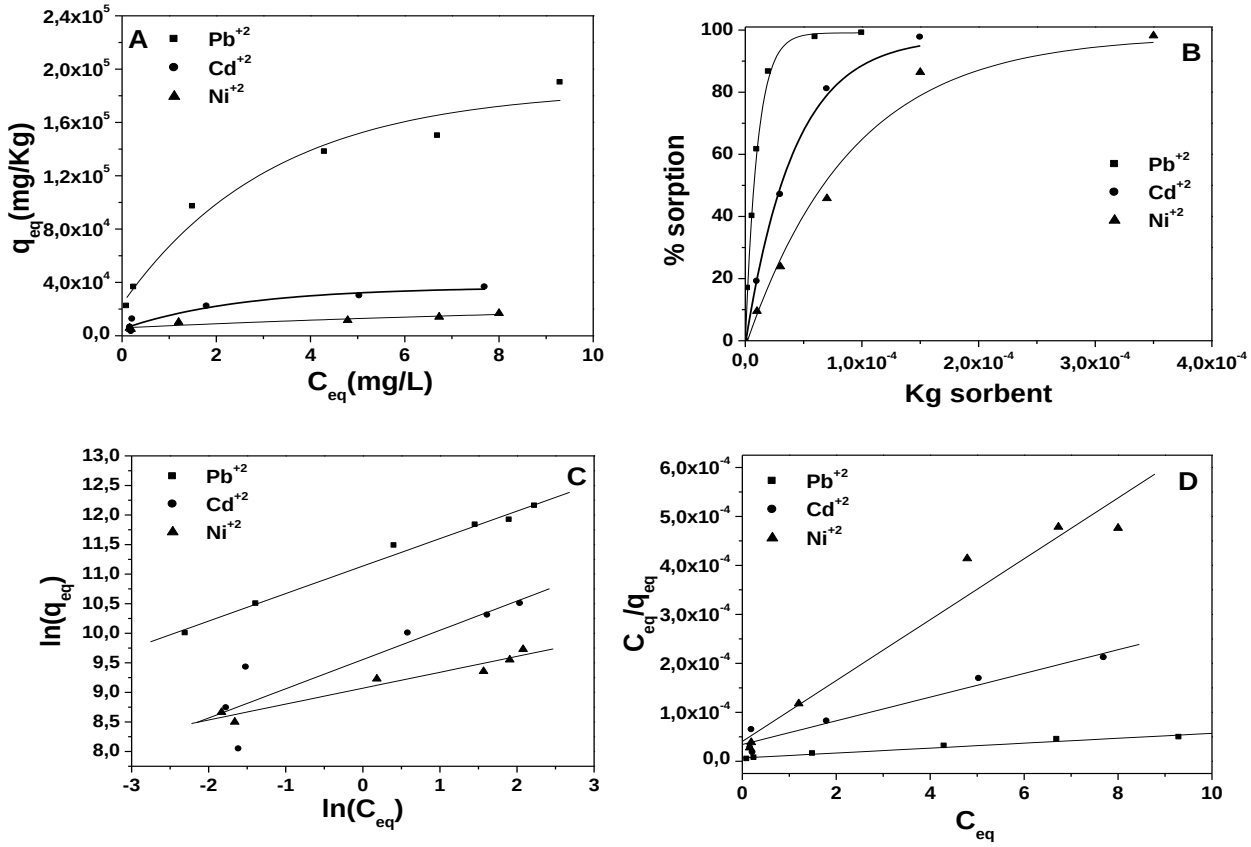

Figure 3. A) Batch tests in de-mineralized water for single solutions of lead, cadmium and nickel ions (1-3 mm BOP particle size, 80 rpm, 10 mgMe^{+2}/L, pH = 6, T = 298 K). B) % sorption Vs sorbent dosage. C) Pb^{+2}, Cd^{+2} and Ni^{+2} Freundlich isotherms. D) Pb^{+2}, Cd^{+2} and Ni^{+2} Langmuir isotherms.

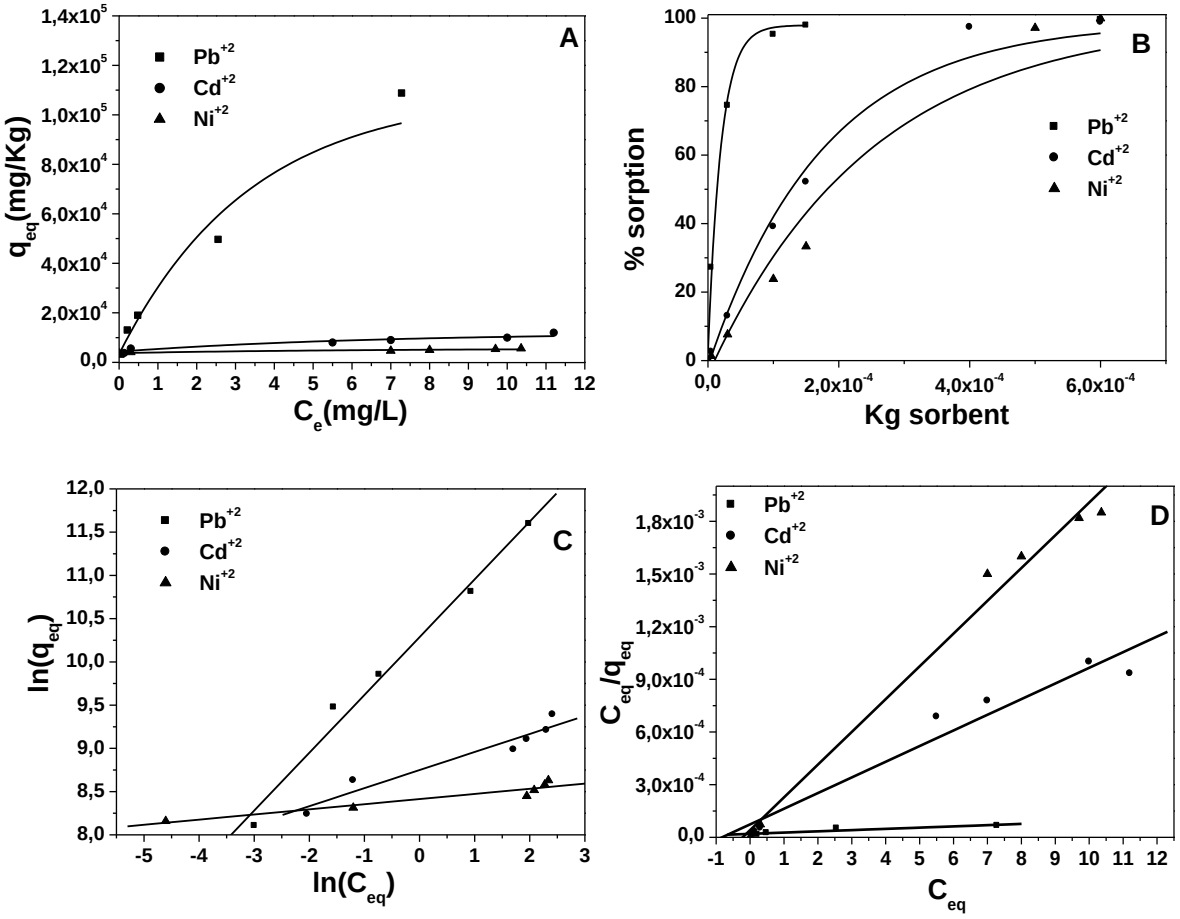

Figure 4. A) Batch tests in de-mineralized water for ternary solution of lead, cadmium and nickel ions (1-3 mm BOP particle size, 80 rpm, 10 mgMe^{+2}/L, pH = 6, T = 298 K). B) % sorption Vs sorbent dosage. C) Pb^{+2}, Cd^{+2} and Ni^{+2} Freundlich isotherms. D) Pb^{+2}, Cd^{+2} and Ni^{+2} Langmuir isotherms.

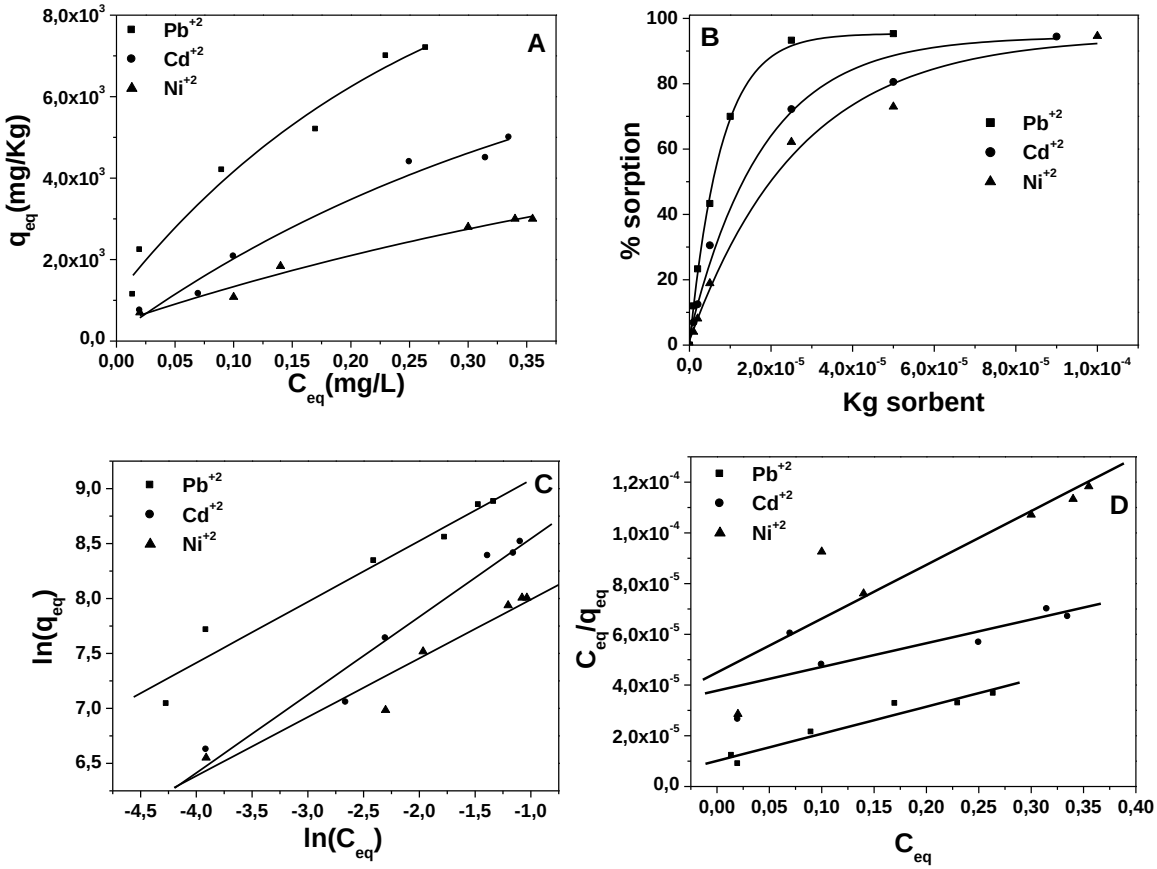

Figure 5. A) Batch tests in tap water for ternary solution of lead, cadmium and nickel ions (1-3 mm BOP particle size, 80 rpm, 0.3 mgMe^{+2}/L, pH = 7.5, T = 298 K). B) % sorption Vs sorbent dosage. C) Pb^{+2}, Cd^{+2} and Ni^{+2} Freundlich isotherms. D) Pb^{+2}, Cd^{+2} and Ni^{+2} Langmuir isotherms.

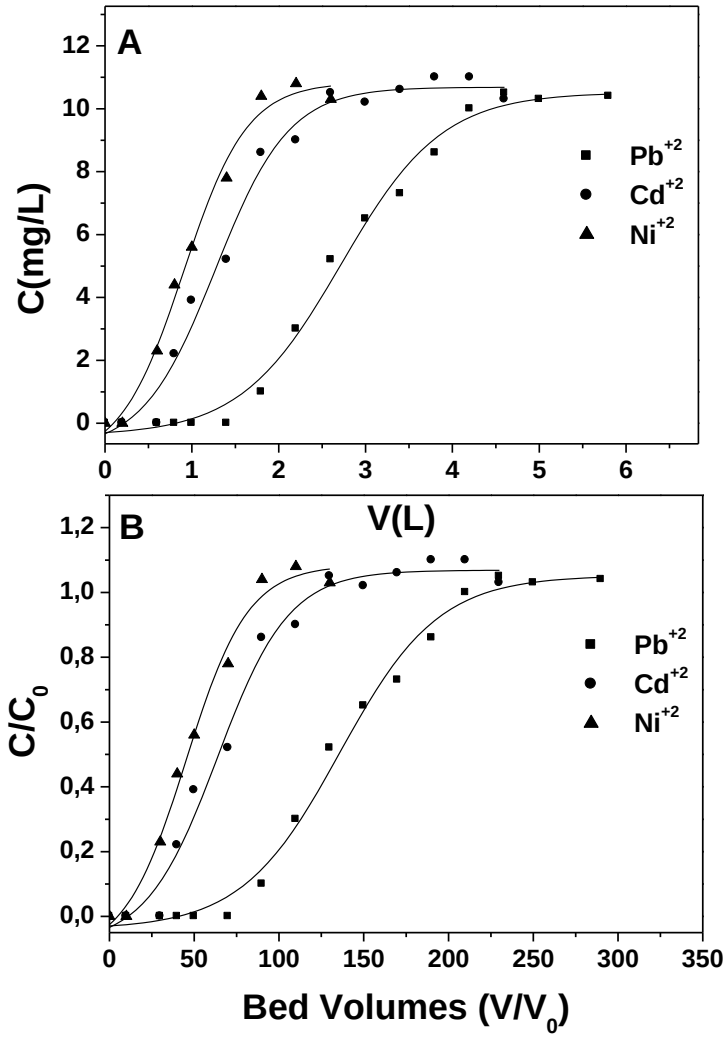

Figure 6. A) and B) Breakthrough curves in de-mineralized water for solution of lead, cadmium and nickel ions on BOP (1-3 mm particle size, 0.7 L/h, 10 mg Me^{+2}/L, pH = 6, T = 298 K).

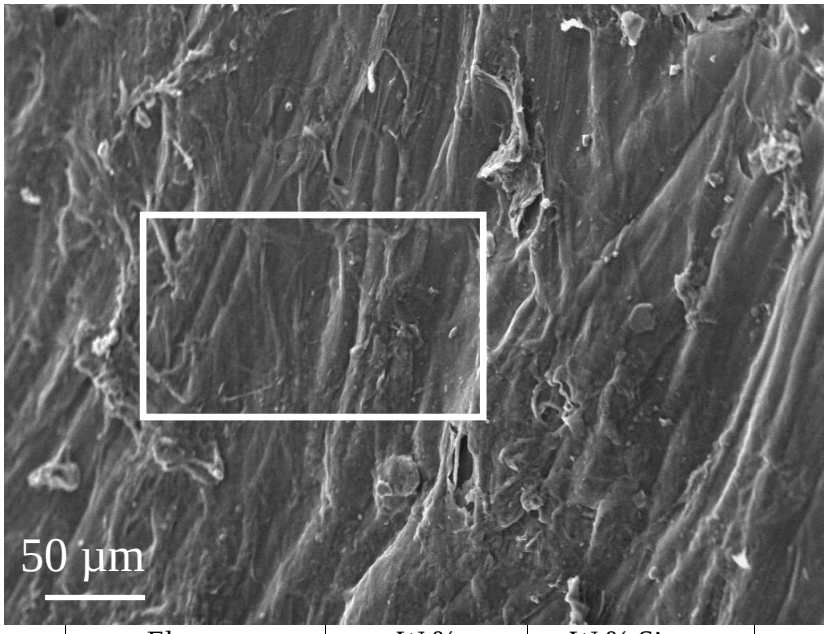

Element	Wt%	Wt% Sigma
Ni	13.84	0.83
Cd	19.41	1.09
Pb	46.79	1.39

Figure 7. EDX analysis of metal laden BOP after column test in ternary solution (5.5 g BOP, 0.7 L/h, 10 mg Me^{+2}/L influent ternary solution, pH = 6, T = 298 K).